

The effect of different initial conditions on the exit flow from a fluidic precessing jet nozzle

by

C.Y. Wong^{1,a}, G.J. Nathan^{1,b} and T. O'Doherty^{2,c}

¹ University of Adelaide
Mechanical Engineering Department
North Terrace, Adelaide, South Australia 5005

² University of Wales
School of Engineering, Division of Mechanical Engineering
Cardiff, Wales, United Kingdom, CF24 OYF

^aE-Mail: cwong@mecheng.adelaide.edu.au

^bE-Mail: gnathan@mecheng.adelaide.edu.au

^cE-Mail: Odoherty@Cardiff.ac.uk

ABSTRACT

The fluidic precessing jet (FPJ) shown in Figure 1 is one of a family of self-excited oscillating jet flows that has found application in reducing Oxides of Nitrogen (NO_x) from combustion systems in the high temperature process industries. Its flow field is highly three-dimensional and unsteady, and many aspects of it remain unresolved. Velocity data measured close to the exit plane is presented for a variety of FPJ nozzles with three different inlet conditions, namely a long pipe, a smooth contraction and an orifice. The results indicate that jet inlets which are known to have asymmetrically shedding initial boundary layer, such as that produced by either an orifice or a pipe, trigger jet precession more easily than jet inlets which are known to have symmetrically shedding initial boundary layers. Although the exit flow is dominated by the reliability with which a given configuration generates precession, the three different inlet conditions also produce subtle differences in the exit profiles of mean velocity and turbulence intensity when the flow does precess reliably.

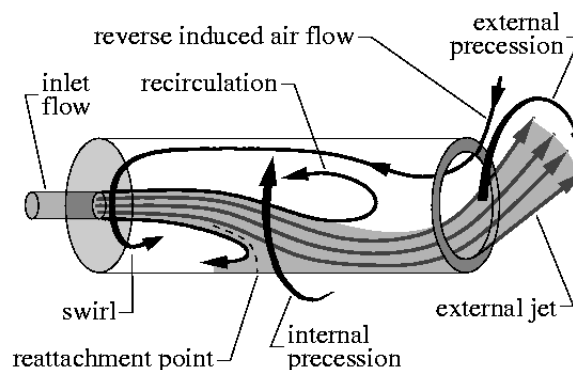


Fig. 1. A simplified representation of the flow in a fluidic precessing jet nozzle inferred from flow visualization

1. INTRODUCTION

The Fluidic Precessing Jet (FPJ) nozzle shown in Figure 1 has found application as a burner for rotary cement and lime kilns. The FPJ burner has demonstrated reduced NO_x emission relative to conventional burners, significant fuel savings and an improvement in product quality ((Manias and Nathan, 1994, and Manias *et al.*, 1996). Since its discovery (Nathan, 1988) and subsequent patent (Luxton *et al.*, 1991) much research has been invested to study the behaviour of this naturally oscillating jet flow. Research in the last decade has focused on the external mixing field of a wide range of precessing jet nozzles, including those that closely resemble the industrial configurations. Measurements have been performed under both isothermal and reacting conditions.

The FPJ nozzle in its simplest form is a cylindrical chamber with a small axisymmetric inlet at one end and an exit lip at the other. The inlet flow separates at the inlet and reattaches asymmetrically to the wall of the chamber. A rotating pressure field is established within the chamber which causes the reattaching flow to precess around the inside wall of the chamber and this also produces a precessing exit flow (Nathan *et al.*, 1998). The lip and large transverse pressure gradients near to the outlet steer the exit flow through a large angle towards the axis and across the face of the nozzle outlet as shown in Figure 1. The emerging flow is highly three-dimensional and unsteady, with both the exit angle and precession frequency exhibiting considerable cycle-to-cycle fluctuations. This renders measurement difficult.

Various inlet flows to the nozzle have been used previously including a “top-hat” velocity distribution produced by a contoured nozzle inlet, a pipe flow velocity distribution and a flow from a sharp edged orifice which results in a vena contracta being formed just downstream of the sharp edge. Nathan (1988) showed that each of these inlet flows can produce precession and deduced that the presence or absence of precession dominated the characteristics of the exit flow. However, the scope of that investigation did not include quantification of these details.

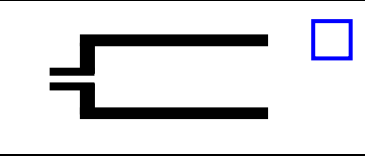
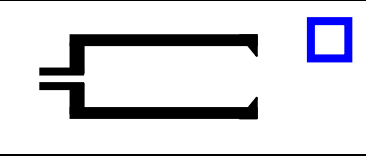
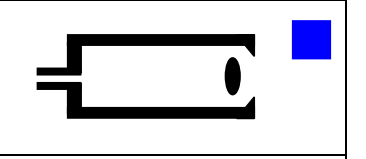
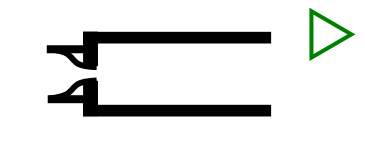
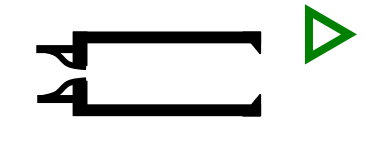
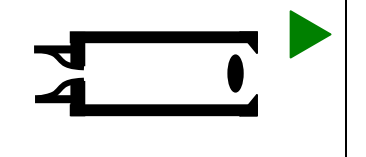
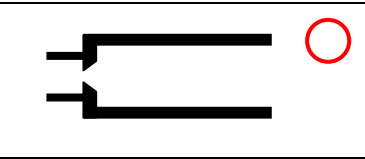
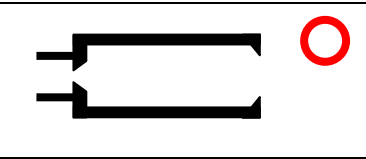
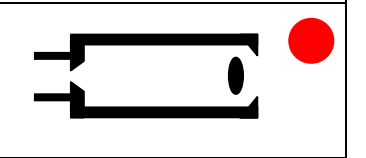
Mi *et al.* (2001) have shown that in an unconfined jet, the three different inlet conditions above produce significantly different near-field turbulent flow structures, and that these differences propagate into the far-field. They have observed that contoured nozzles produces relatively large and fairly symmetric roll-up structures in the near field. While the sharp edged orifice inlet also generates distinct, although smaller, roll-up structures they tend to be shed asymmetrically. In contrast, the pipe jet inlet produces less evidence of large-scale organised motions although smaller roll-ups are observed to be randomly formed around the jet periphery. These issues provide the motivation for the present investigation. This paper seeks to quantify the effect of inlet conditions on the resulting precessing jet flow in terms of axial, radial and tangential velocities and frequency of precession for each of three different nozzle configurations.

2. EXPERIMENTAL DETAILS

2.1 Types of configurations used

The study assessed three inlet conditions for each of three nozzle configurations shown schematically in Table 1. The chamber configuration is shown on the abscissa and the inlet on the ordinate. The colours and symbols shown in Table 1 are used consistently throughout subsequent figures. The notation combines the labels in the abscissa and ordinate. For example, the notation Pipe (Ch,L,CB) refers to the top right case. Further details for these nozzles can be found in Wong *et al.* (2001).

Table 1. Schematic diagrams of the various configurations of precessing jet nozzles examined in the experiment along with the symbols and notations used to represent them in subsequent figures.

Pipe			
Contraction			
Orifice			
	Open Chamber (Ch)	Chamber and Lip (Ch, L)	Chamber, Lip and Centrebody (Ch, L, CB)

2.2 Experimental Set-up

2.2.1 Air supply and seeding

Laser-Doppler anemometry (LDA) measurements were conducted at the Mechanical Engineering Department at the University of Wales, Cardiff. A mains compressor with a capacity of 4000 l/min at 600 KPa supplied air to the experimental nozzles used in the experiment. The compressed air is channelled through a 2000 l/min flowrator, followed by a seed ejector. The seed ejector entrained sub-micron “HAZE” glycol particles produced by an external ROSCO 4500 fog generator. These particles had diameters less than 1 μm and a density ratio relative to air of 800. Their frequency response has been estimated by Melling and Whitelaw (1975) and Durst *et al.* (1975) using an approximate equation derived from Stokes equation and was found to be up to 7.35 KHz, which is more than adequate for the present investigation. At this maximum frequency, the ratio of the amplitude of such a particle’s oscillation to amplitude of fluid oscillation is greater than 0.99. This meant that the particles used were sufficiently small to follow the flow with negligible time lag. The outlet from the seed ejector is connected to a long flexible hose. This, in turn, is coupled to either a long pipe or a flow conditioner for the smooth contraction and orifice inlets. Part of the fog is divided to seed the entrained ambient flow so that there is seeding of both the surrounding ambient fluid and the jet fluid. This is to alleviate a bias towards higher velocities if only one flow is seeded (Durst *et al.*, 1981). The experimental arrangement is shown schematically in Figure 2. This arrangement does not allow the flowmeter to directly measure the total flowrate through the nozzle, thus resulting in different Reynolds number for each configuration tested. However, the actual flow through the nozzle was quantified for each case by velocity profiles at the nozzle inlet plane.

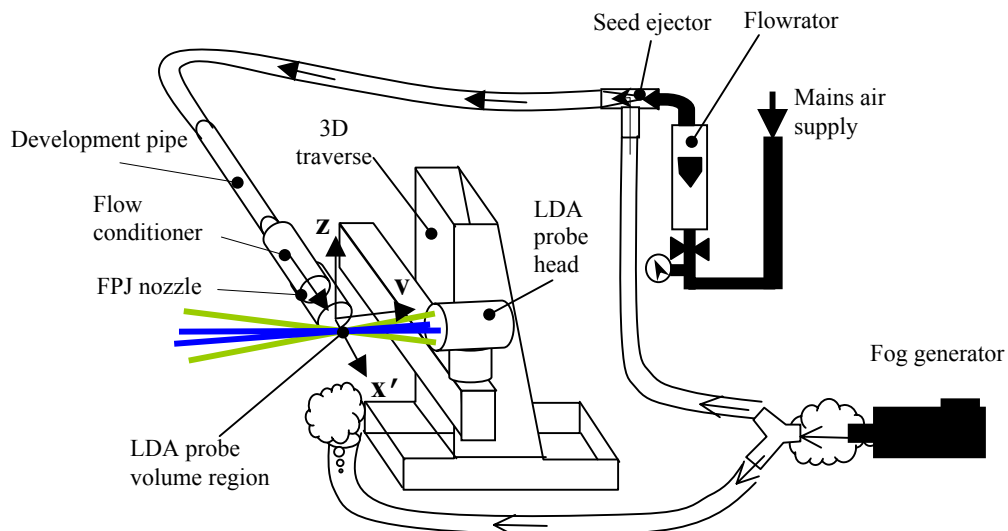


Fig. 2. A schematic diagram of the experimental arrangement. For clarity, the light generation system, burst spectrum analysers and the support for the flow conditioner are not shown.

2.2.2 Flow conditioner

Flow conditioning is achieved first by a development pipe of 30 diameters in length connected in series to a diffuser that has an included angle of 9.1° and an expansion area ratio of 2.1. This is followed by a honeycomb section which has a length-to-diameter ratio of about 12 to reduce any upstream swirl. A series of 5 screens, each with an open area ratio of 61% and screen diameter of 0.355 mm is used to further improve the flow uniformity and reduce the turbulence intensity of the flow. A development section equivalent to about 280 wire diameters follows immediately after the last screen to allow any vortical structures generated by the screens to dissipate. Further details can be obtained in Wong *et al.* (2002).

To obtain a “top-hat” velocity profile at the FPJ inlet plane, a nozzle with a 5th order polynomial profile with zero derivative end conditions and a contraction area ratio of 10.03 is attached to the end of the development section. Alternatively, a 5 mm thick sharp-edged orifice plate with a downstream chamfer of 45° is attached to the end of the development section which generates a vena contracta downstream from the sharp edge. To obtain a pipe flow inlet, a length of about 100 pipe diameters was used. All the internal diameters, d , of the inlets were kept the same at 15.79 mm.

2.2.3 Laser-Doppler Anemometer

The two-component laser-Doppler anemometer uses the 514.5nm (Green) and 488.0nm (Blue) lines from a 5 Watt Innova 70 Coherent Argon-ion laser. Each colour is split, with one beam from each pair being frequency shifted by 40MHz using a Bragg Cell to remove directional ambiguity. Clock-induced bias due to the frequency shift is corrected following Graham *et al.* (1989). A fibre-optic system for collection in back-scatter mode is used for delivery and collection with a beam spacing of 64mm and a focal length of 310 mm. The ellipsoidal probe volume has a length of 1.65 mm and a nominal waist diameter of 0.170 mm for the green beam and 1.57 mm by 0.162 mm for the blue beam. The average probe length is about 2% of the FPJ nozzle diameter. This probe is traversed by a Dantec 3-axis traverse system that has a position accuracy of 0.05mm in three orthogonal directions. One axis of the traverse is aligned parallel to the axis of the nozzle as shown in Figure 2. Time-averaged measurements were performed in burst-and-coincidence mode to provide simultaneous two-component velocity measurements, while the Burst Spectrum Analyser (BSA) was programmed to collect up to 10,000 velocity samples. The time window for coincidence was set at 1 millisecond, while the time-out for incoming data record was set to 200 seconds.

2.3 Procedure

The LDA probe volume was positioned at $x'/d=0.63$ downstream from the nozzle exit plane (Figure 3). Measurements were performed at 46 locations equally spaced at 2 mm across the entire exit plane for all nine configurations (Table 1). When measuring the axial component of velocity (u), the blue beam pair was used. The green beam pair was used to measure the radial (v) and tangential (w) velocity components. The green beam pair has a higher energy distribution than the blue beam pair and is better at resolving the motion of weakly scattered seed particles usually moving in a direction perpendicular to the bulk flow (i.e., the tangential and radial components). In measuring the axial and radial components, the probe was traversed along the y -axis. Similarly, to acquire the axial and tangential components, the probe was moved along the z -axis.

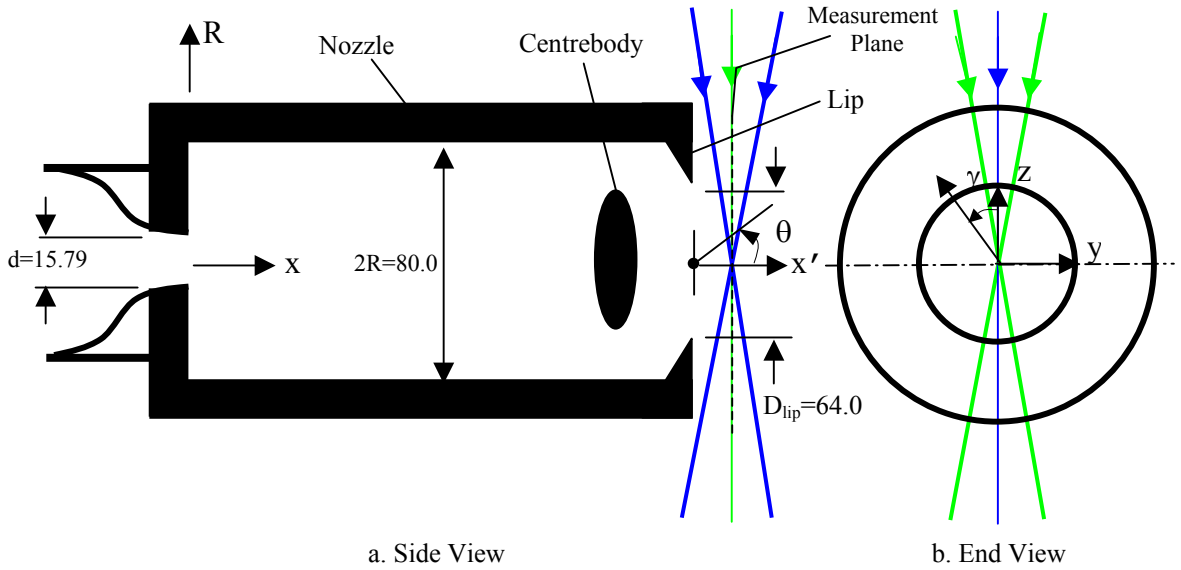


Fig. 3. The coordinates and dimensions of the FPJ nozzle. Mean velocities in x (or x'), z and y directions are represented as u , v and w respectively in the text and graphs. Root-mean-squared (r.m.s.) values are similarly represented as u' , v' and w' respectively. All dimensions in mm.

3. RESULTS AND DISCUSSION

3.1 Inlet flows

Table 2 summarises the conditions at which the inlet flow distributions were obtained. The initial velocity profiles were measured for the 3 jets in an unconfined environment, i.e. with the chamber removed. This avoids the optical distortion associated with the chamber (Wong *et al.*, 2001) and also allows comparison with other investigations. Fig. 4 and 5b shows that the velocity distributions for the three inlet flows are quite symmetrical with the expected mean and r.m.s profiles reported in literature. The velocity profile for the jet exiting the pipe is comparable to the profile described empirically by a power-law equation (shown in Fig. 4a) and the boundary layer is in a fully turbulent state. Its turbulence intensity at the centreline and shear layer is about 4.2% and 15% respectively. The flow emerging from the smooth contraction is described to have a nearly “top-hat” velocity profile (Fig. 4b) similar to that of Crow and Champagne

(1971) (who measured at $x/d=0.025$) and is known to be in a laminar flow state. Its turbulence intensities at the centreline and at the shear layers are 1.6% and 18% respectively. Fig. 5a shows the near-field centreline axial velocity decay of the orifice jet. This result compares well with the hot wire measurements of Quinn and Miltzer (1989). For the present experiment, the highest axial velocity was obtained around $x/d=2.6$, which is representative of the flow in the region of the vena contracta. Fig 5b shows that the mean velocity profile is similar to that of Quinn and Miltzer (1989). At $x/d=2.67$, Quinn and Miltzer (1989) reported a centreline and shear layer turbulence intensity of 4.7% and 15% respectively. This is comparable with the turbulence intensity of the present measurements for the orifice at 4.1% and 17% respectively. The origin for the far-field decay is slightly upstream in the present jet, possibly due to slight differences in the chamfer of the orifice or the differences in Reynolds number.

Table 2. Conditions at which velocity distributions of the respective inlets were obtained.

Type of Inlet	Bulk Velocity m/s	Reynolds Number	No. of axial jet diameters downstream from jet exit plane
Pipe	36.6	39,300	0.34d
Contraction	40.1	43,100	0.56d
Orifice	53.0	56,900	2.60d

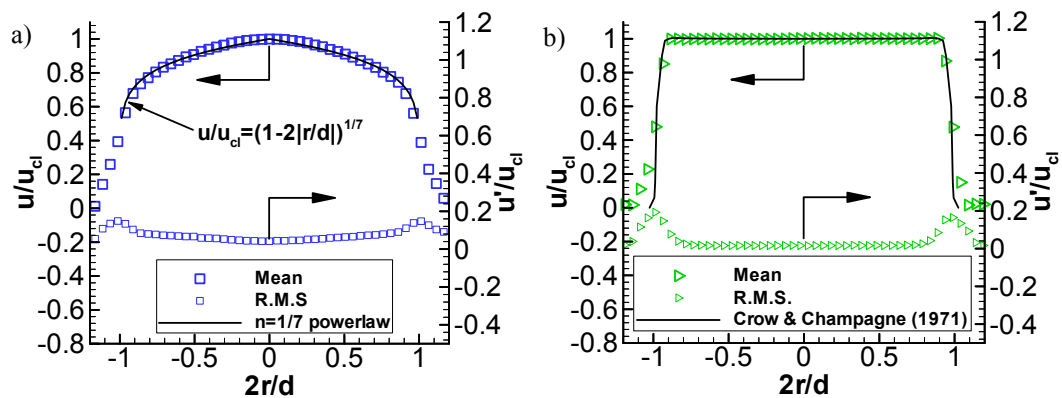


Fig. 4. Axial mean velocity (u) and r.m.s. (u') distributions of the pipe(\square) and contraction(\blacktriangleright) jet inlets. All values are normalised with the centreline velocity, u_{ci} .

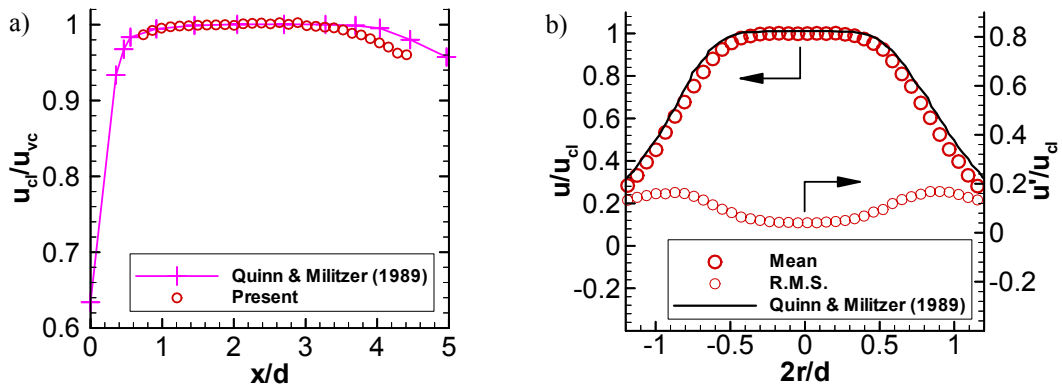


Fig. 5. a) Axial location of the vena contracta for the present orifice(\circ) jet compared with literature data. b) Axial mean velocity (u) and r.m.s. (u') distribution with values normalised to centreline velocity, u_{ci} . Re of the present jet is at 56,900 based on d and the bulk velocity at $x/d=2.60$. Re for Quinn and Miltzer (1989) is 208,000 based on the bulk inlet velocity. u_{vc} is the mean velocity in the region of the vena contracta.

3.2 Time-averaged measurements

The measurements of the flow through the FPJ nozzle were all performed with an inlet Reynolds number of greater than 80,000 to ensure they were fully turbulent. It is recognised that velocity corrections (such as inverse velocity weighting by McLaughlin and Tiederman (1973)) are needed for these measurements due to various forms of biases. However, the methods, which have been outlined by Durst et al. (1981) are varied and it is beyond the scope of this paper to explore them. As such, the data presented in this paper are not in any way corrected to account for velocity bias. In addition, to account for variations in the inlet

velocity for the different configurations, the results at the exit plane are normalized to the mean exit velocity. Table 3 summarises these inlet conditions.

Table 3. Summary of inlet conditions used for the FPJ nozzles.

Type of Inlet	Bulk Velocity, u_i m/s	Reynolds Number Based on u_i at $x/d=1$ and d
Pipe	75.8	81,420
Contraction	162.8	174,872
Orifice	124.7	133,946

The exit flows are presented in Fig. 6 for the Chamber, in Fig. 7 for the Chamber and Lip, and in Fig. 8 for the Chamber, Lip and Centrebody cases. The characteristic differences associated with each general configuration are considered first and subsequent sections will address the differences associated with each inlet.

The chamber alone can be seen to produce a mean exit axial velocity profile (Fig. 6a) with a characteristic bell-shape. For the chamber and lip, two of the three mean exit profiles are quite different with a double peak showing the jet emerging from the outside of the nozzle (Fig. 7a). With the centrebody as well, the double-peak in the mean profile is very consistent and occurs for all inlet types (Fig. 8a). These differences can be explained by the dynamics of the flow investigated previously. Nathan *et al.* (1998) showed that the flow in the chamber is bi-modal, and switches between an axial jet (AJ) and a precessing jet (PJ) mode. They also showed that the presence of the lip greatly favours the precessing mode over the axial mode. The “bell-shape” in the mean profiles can therefore be associated with the AJ mode, while the double-peak profile is associated with the PJ mode. As described earlier and shown in Fig. 1, when in the PJ mode the flow at any instant leaves from only one “side” of the chamber so that the double-peak is in the time-mean, but not the phase-mean, or instantaneous profiles. The phase-mean distribution of the axial velocity component in the emerging plane has been quantified by Wong *et al.* (2002) and has the peak on only one side of the axis.

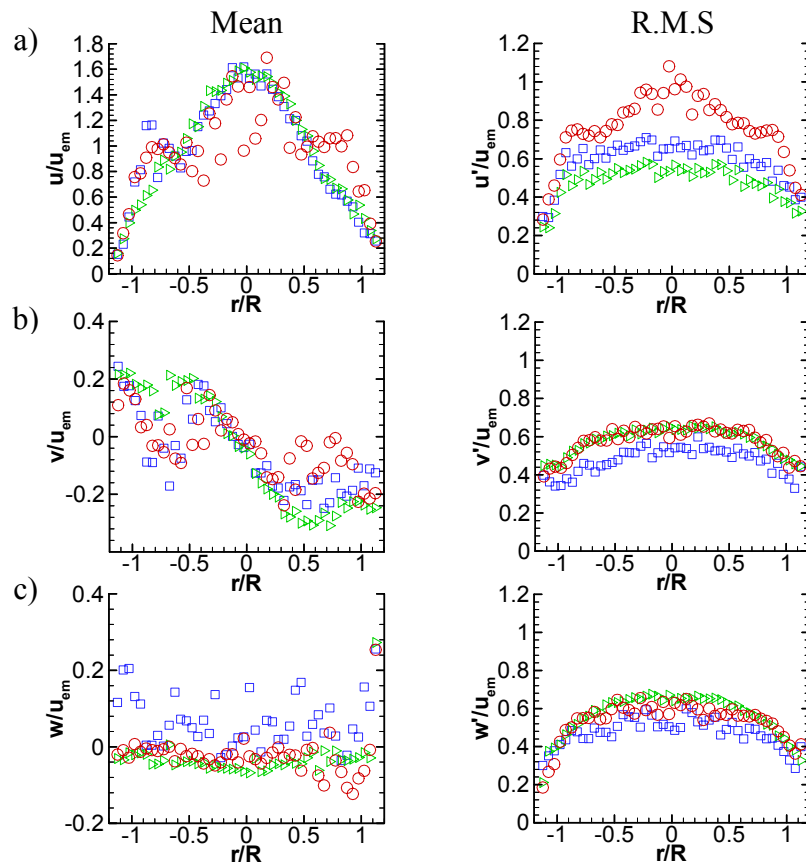


Fig. 6. Time-averaged mean and r.m.s. velocity profiles for chamber only case. a) Axial, b) Radial and c) Tangential. All values are normalised with the average axial velocity, u_{em} of each case. Symbols as per Table 1.

The radial profiles of the axial r.m.s. also exhibit a strong dependence on the flow mode. The r.m.s. of those cases corresponding to the axial mode with the bell-shaped mean profile is much lower than those associated with the precessing mode and the double peak in the mean profile. For example, $v'/u_{em} \sim 0.5$ for pipe (Ch) and contraction (Ch) (Fig. 6a) compared with $v'/u_{em} \sim 1$ for pipe (Ch, L, CB) and contraction (Ch, L, CB) (Fig. 8a). A higher r.m.s. would be expected with the oscillating motion associated with the precessing emerging flow (Nathan *et al.*, 1998 and Wong *et al.*, 2002).

3.2.1 The effect of initial conditions on the Chamber configuration

Fig. 6 presents the mean and r.m.s. velocity at the exit plane for the chamber only configuration, ie. without the lip or the centrebody. Examining the mean axial components in Fig 6a, it is clear that the orifice inlet exhibits significantly different behaviour to the smooth contraction and pipe. Where the latter two have the distinct bell-shaped profile associated with the AJ mode, the orifice exhibits both considerably more scatter and has three peaks. This is consistent with the flow switching intermittently between the two modes so that in the mean, the double peaks are super-imposed on the bell-shape in the curve. The higher r.m.s. in the orifice data is also consistent with mode switching. Together, these data suggest that the orifice inlet is more conducive in generating the PJ mode than the smooth contraction or pipe case.

In addition, the pipe inlet can be seen to exhibit a slight tendency to produce the precessing jet mode with one weak side-peak in the mean profile and a slightly higher r.m.s., than the smooth contraction. This trend in the r.m.s. is opposite to what would be expected for the free jet cases, where the smooth contraction has a higher r.m.s. than the pipe (Mi *et al.*, 2001). Hence Fig.6 further suggests that the pipe jet is more conducive to generating the PJ mode than the smooth contraction.

3.2.2 The effect of initial conditions on the Chamber and Lip configuration

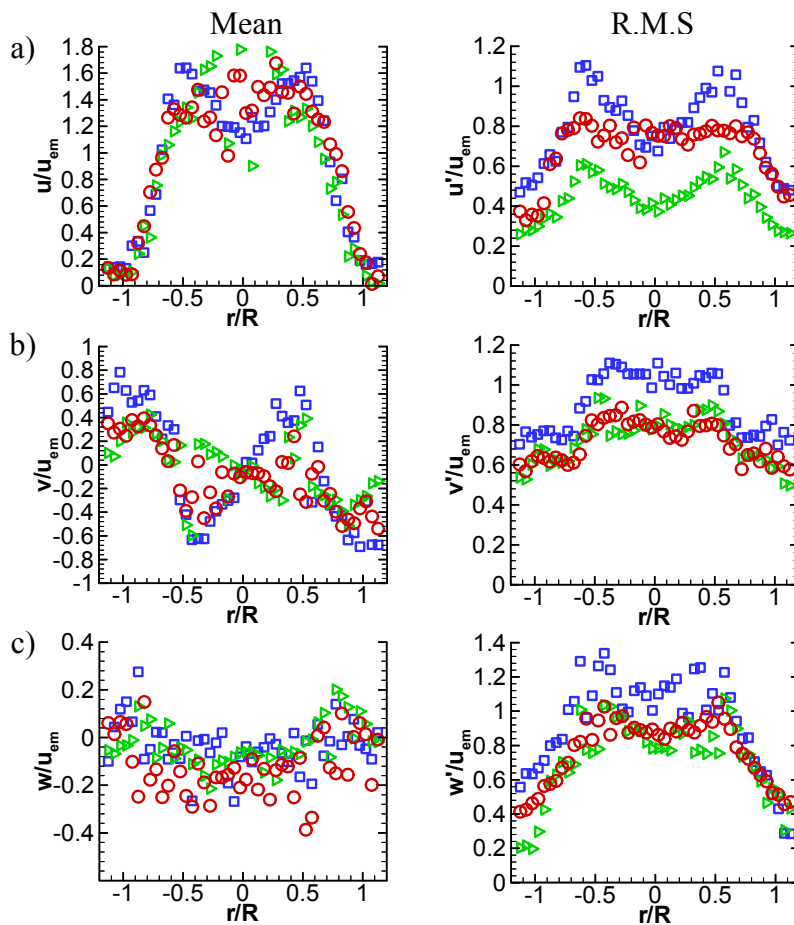


Fig. 7. Time-averaged mean and r.m.s. velocity profiles for chamber and lip case. a) Axial, b) Radial and c) Tangential. All values are normalised with the average axial velocity, u_{em} of each case. Symbols as per Table 1.

Adding a lip to the chamber promotes the predominance of the PJ mode (Nathan *et al.*, 1998) and this is characterised by the increased significance of the double peak in the mean exit profile (Fig 7a). Both the orifice and pipe inlet show a dominant PJ mode, while the smooth contraction shows a dominance of the AJ mode. This is consistent with the trend noted in Fig 6. The radial r.m.s. profiles in Fig 7b also exhibit the double peak, unlike Fig. 6. This is consistent with the dominance of the precessing mode resulting in the oscillation of the emerging precessing jet. In one phase in the cycle, the jet has high radial velocities in one direction, while at the opposite phase, the direction is the opposite (Wong *et al.*, 2002). The tangential mean and r.m.s. velocities in Fig 7c for all inlet cases indicate that the precessing jet does not have a preferred mean direction when exiting the chamber. This is consistent with the conservation of angular momentum, which is zero, at the nozzle inlet plane. Nevertheless, the emerging jet does appear to have a strong tangential component since tangential r.m.s. profiles exhibit double peaks with about the same location and intensity as the axial components.

3.2.3 The effect of initial conditions on the Chamber, Lip and Centrebody configuration

The centrebody has a big influence on the flow-field, reducing the variability in the exit flow with different inlet conditions, as shown in the good collapse of the mean velocities in Fig. 8a and the improved collapse in Figures 8b and 8c. The flow also emerges more strongly from the edge of the nozzle just within $|r/R|=0.64$, as has been shown in the phase-averaged measurements of Wong *et al.* (2002). Nevertheless, the inlet flow does have a secondary influence on the emerging flow. The orifice inlet produces the highest exit r.m.s. for all three components, while the pipe produces the lowest (Fig. 8a). This is the same trend as occurs in a free jet (Mi *et al.*, 2001), suggesting that these effects are superimposed on the now dominant precessing motions. The introduction of the centrebody also serves to bias the mean azimuthal direction of the precessing jet, as shown in Fig. 8c (mean). However, the peak in the mean tangential component is not consistent with the peaks in the axial and radial components, but rather occurs at a greater radius. Indeed, it is coincident with the weaker outer peaks in the radial component, suggesting it may be associated with the induced ambient fluid.

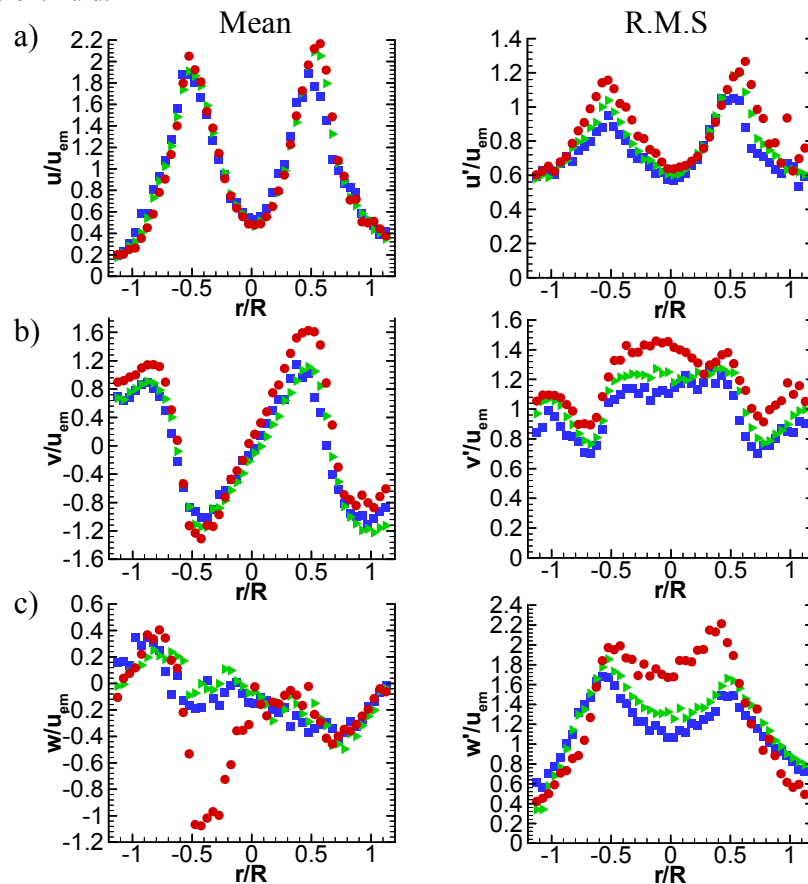


Fig. 8. Time-averaged mean and r.m.s. velocity profiles for chamber, lip and centrebody case. a) Axial, b) Radial and c) Tangential. All values are normalised with the average axial velocity, u_{em} of each case. Symbols as per Table 1.

3.3 Frequency analysis of the various FPJ nozzles

The precession frequency, f_p , for each case is estimated from the axial velocity frequency spectrum obtained near $r/R=0.62$ at a probe location used by Nathan *et al.* (1998) to detect precession. These measurements are presented in Fig. 9 as arbitrary energy spectrum, whereby the time series velocity data are re-sampled using linear interpolation with the maximum frequency determined by half the mean data rate.

The Chamber-only (Ch) configurations do not show distinct low frequency peaks in their spectrums, but rather, a gradual “hump”. This supports the deductions that the AJ mode is dominant in this type of configuration. All other configurations show distinct spectral peaks around 10 Hz associated with jet precession occurs (Nathan *et al.*, 1998). However, further analysis of other spectral data shows that the axial jet mode occurs more frequently than the precessing jet mode in the Contraction (Ch, L) case.

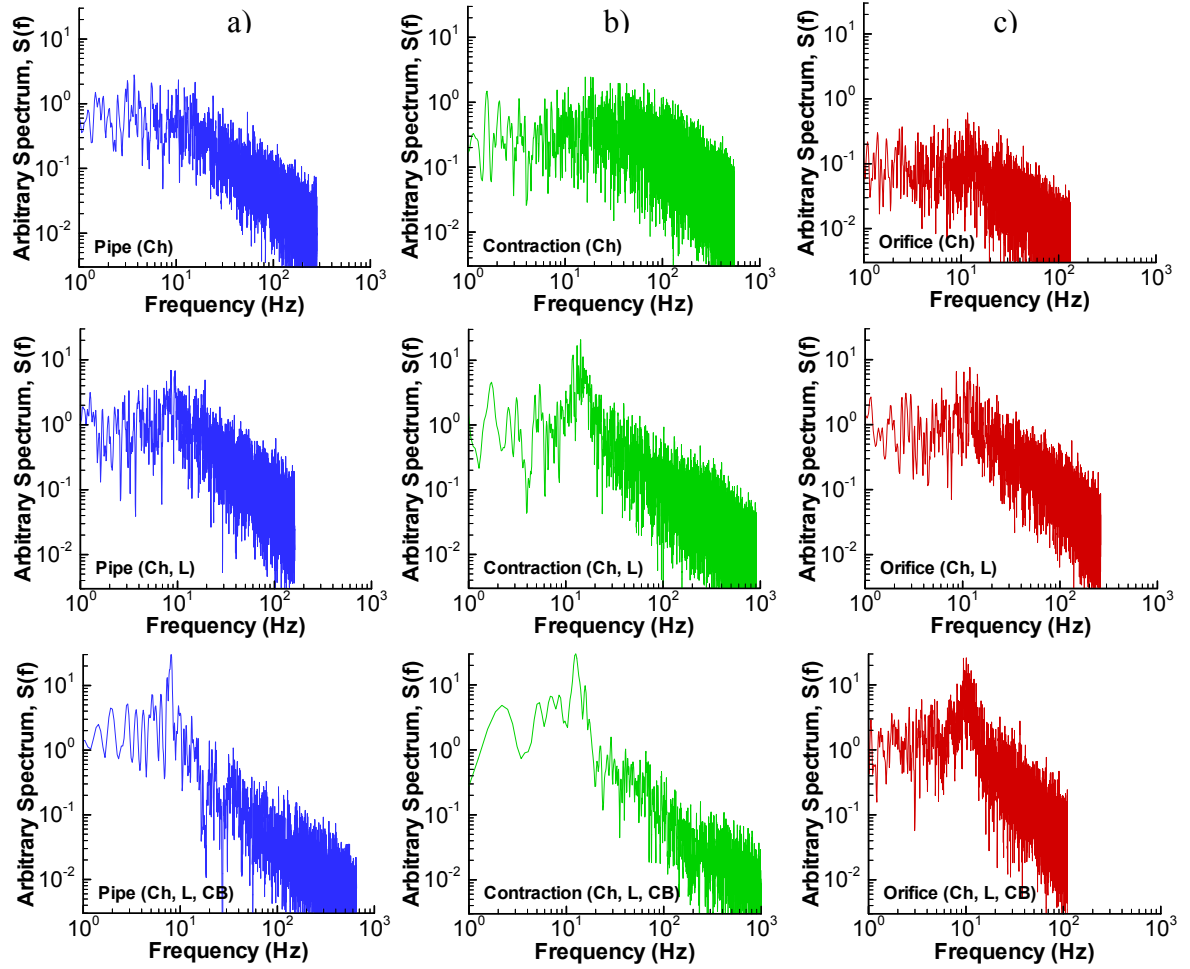


Fig 9. Log-log arbitrary spectral energy plots of the various configurations at $r/R=0.62$. Notation as per Table 1. a) Pipe inlet, b) Contraction inlet and c) Orifice inlet.

A non-dimensional Strouhal number, St , can be used to compare these precession frequencies with those in literature. Since not all configurations have a dominant precession frequency, as discussed above, only those configurations that do show distinct frequency peaks are presented. The Strouhal number can be calculated using equation (1), where $h = (D-d) / 2$ and $u_i =$ bulk inlet velocity, following Nathan *et al.* (1998).

$$St = \frac{f_p \times h}{u_i} \quad (1)$$

The Strouhal number is then plotted against Reynolds number, Re , defined by equation (2), where d = inlet diameter and ν = kinematic viscosity. The plot is shown in Fig. 10.

$$Re = \frac{u_i \times d}{\nu} \quad (2)$$

The reliability of the present measurement is established by the good agreement of the present measurement of the orifice (Ch, L) configuration with an expansion ratio, $E=5.0$ with the comparable measurement of Nathan *et al.*(1998) (N98). The slight difference may be caused by the different expansion ratio, $E=6.43$ in the latter.

The trend of a slight decrease in St with increasing Re was observed by Nathan *et al.* (1998). The results, shown in Fig. 10, indicate that FPJ nozzles with centrebody arrangements decrease St slightly in every case. It is not conclusive whether St depends on the present initial conditions as each configuration was assessed at a different Reynolds number (see Section 2.2). However, the similar trend in the present data relative to that of Nathan *et al.* (1998) suggests that any influence of initial condition on St is small.

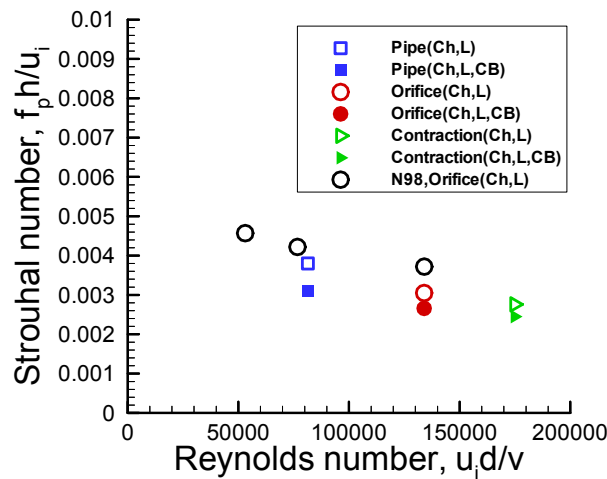


Fig. 10. Strouhal number versus Reynolds number plot of the various FPJ configurations compared with literature data.

4. DISCUSSION

The present work shows that the inlet flow significantly influences the relative dominance of the PJ and AJ flow modes, with the orifice favouring the PJ mode the most and the smooth contraction the least. This is deduced to be associated with the degree of instantaneous asymmetry in shedding of the boundary layer from the nozzle. This is in agreement with the findings of Mi *et al.* (2001) and the postulation by Nathan *et al.* (1998) that natural instantaneous asymmetry within the jet is significant in generating precession.

Mi *et al.* (2001) examined the initial flow structure from these three initial conditions in a free environment and showed that their initial structures are quite different. They showed that the initial structure in a jet from a smooth contraction is highly coherent and symmetrical, while that from an orifice is somewhat less coherent and asymmetric. The initial structure from a pipe is different again (Mi *et al.*, 2001), with less evidence of visually coherent large-scale organised motions but rather smaller scale and more random motions. They added that for the orifice, strong recirculation regions exist both upstream and downstream from the orifice plate, while no upstream separation exists for the smooth contraction. Other authors, such as Reeder and Samimy (1996) and Zaman (1999) have used small tabs at the edge of a contoured nozzle to generate an initially asymmetric shear layer. They found that such tabs increase jet mixing and entrainment substantially.

Quinn (1990) has examined the flow of a free jet from an asymmetric (triangular orifice) inlet and found that its Reynolds shear stress levels are higher than that from a smooth contraction inlet. He reasoned that

the higher shear stress levels promoted mixing. Recently, Lee et al. (2001), have used a triangular orifice for an inlet condition expanding suddenly into a short chamber and they concluded that the use of an asymmetric (triangular) jet inlet with a larger equivalent diameter allows dominant jet precession (PJ mode) to occur for a wider range of Reynolds number and configurations than the present configurations presented. The evidence suggest that having a shear layer that is highly three-dimensional at the initial inlet to the FPJ nozzle not only provides rapid mixing in the near-field but also triggers and promotes jet precession more easily than an initial shear layer that is axisymmetric. Taken together, these findings support the hypothesis of Nathan *et al.* (1998) that instantaneous asymmetries within the turbulence structure of the jet are important in the generation of the PJ mode.

5. CONCLUDING REMARKS

The initial conditions of the jet entering the nozzle chamber contribute significantly to the flow within and emerging from an FPJ nozzle. Inlet conditions have a significant influence on the relative dominance of the precessing jet (PJ) or axial jet (AJ) mode. Those inlets which favour asymmetric shedding of the initial boundary layer and turbulent structures, such as that produced by either an orifice or a pipe, trigger jet precession more easily than jet inlets which are known to have symmetrically shedding initial boundary layers, notably the smooth contraction. In this paper, for FPJ with chamber-only and chamber-and-lip configurations, the orifice inlet favours the PJ mode most and the contraction least. This is postulated to occur as a result of the asymmetry of shear layer shedding at the inlet condition as observed by Mi *et al.* (2001). When the PJ mode is dominant, as occurs in the chamber-lip-centrebody configuration, the turbulence intensity is highest for the orifice inlet and lowest for the pipe inlet. This finding is also consistent with the trends in a free jet as noted by Mi *et al.* (2001). This suggests that the turbulence structure at the inlet is superimposed on the precessing motion and propagates to the outlet, at least in part. That is, the effects of initial conditions are superimposed onto the precessing motion of the FPJ flow. This finding has a more general application to other similar types of complex flows such as combustion chambers in jet engines and boiler furnaces to name a few.

Although the present measurements have provided valuable quantitative data and insight into this complex and unsteady flow, they also highlight the limitation of single point measurements. Planar techniques will allow the instantaneous structures to be identified and assist in differentiating between different flow modes. It is therefore planned to conduct stereoscopic particle image velocimetry (Stereo-PIV) measurements to provide more detailed insight into this complex and important flow.

ACKNOWLEDGEMENTS

The first author gratefully acknowledges the support of the OPRS (Overseas Postgraduate Research Scholarship) and AUS (Adelaide University Scholarship). Support for the travel to the University of Wales, Cardiff (UWC) was provided by an ARC International Research Exchange (IREX) grant. He also acknowledges the friendly assistance provided by the staff and postgraduate students of Mechanical Engineering at UWC in the setting up of the experiments and the lively discussions with fellow members of the Turbulence, Energy and Combustion (TEC) group of the Mechanical Engineering Department within the University of Adelaide.

REFERENCES

- Crow, S. C. and Champagne, F. H. (1971). "Orderly structure in jet turbulence", *J. Fluid Mech.*, **48**, pp.547-591.
- Durst, F., Melling, A. and Whitelaw, J. H. (1981). "Principles and practice of laser-Doppler anemometry", (2nd Edition), Academic Press, London.
- Graham, L. J. W., Winter, A. R., Bremhorst, K. and Daniel, B. C. (1989). "Clock-induced bias errors in laser-Doppler counter processors", *Journal of Physics E: Sci. Instrum.*, **22**, pp.394-397.
- Lee, S. K. , Lanspeary, P. V., Nathan, G. J., Kelso, R. M. and Mi, J. (2001). "Preliminary study of oscillating triangular jets", In B. B. Dally, editor, *Proceedings Of The 14th Australasian Fluid Mechanics Conference*, **2**, pp.821-824, Adelaide, Australia, December, 14AFMC Organizing Committee.

Luxton R.E., Nathan, G.J. and Luminis Pty. Ltd. (1991). "Controlling the motion of a fluid jet", USA Letters Patent, No. 5,060,867.

Manias, C. G. and Nathan, G. J. (1994). "Low NO_x clinker production", World Cement, 25(5), pp.54-56.

Manias, C.G., Balendra, A. and Retallack, D. 1996 New combustion technology for lime production, World Cement, 27 (12), pp.34-39.

Melling, A. and Whitelaw, J.H. (1975). "Optical and flow aspects of particles", In Buchhave P. et al., editors, Proceedings of the LDA-Symposium, pp.382-401, Copenhagen, Denmark, December.

McLaughlin, D. K. and Tiederman, W.G. (1973). "Biasing correction for individual realization of laser anemometer measurements in turbulent flows", Physics of Fluids, 16, pp.2082-2088.

Mi, J., Nathan, G. J. and Nobes, D. S. (2001). "Mixing characteristics of axisymmetric free jets from a contoured nozzle, an orifice plate and a pipe", Transactions of the ASME, 123, pp.878-883.

Nathan, G.J. (1988). "The enhanced mixing burner", PhD thesis, Dept. Mech. Engng, University of Adelaide, Australia.

Nathan, G.J., Hill, S.J. and Luxton, R.E. (1998). "An axisymmetric 'fluidic' nozzle to generate jet precession, J. Fluid Mech, 370, pp.347-380.

Quinn, W. R. and Militzer J. (1989). "Effects of nonparallel exit flow on round turbulent free jets", Int. J. Heat and Fluid Flow, 10(2), pp.139-145.

Quinn, W. R. (1990). "Mean flow and turbulence measurements in a triangular turbulent free jet", Int. J. Heat and Fluid Flow, 11(3), pp.220-224.

Reeder, M. F. and Samimy, M. (1996). "The evolution of a jet with vortex-generating tabs: Real-time visualization and quantitative measurements", J. Fluid Mech., 311, pp.73-118.

Wong, C. Y., Lanspeary, P.V., Nathan, G.J., Kelso, R.M. and O'Doherty, T. (2001). "Phase averaged velocity field within a fluidic precessing jet nozzle", In Proceedings of the 14th Australasian Fluid Mechanics Conference, 2, pp.809-812, Adelaide, Australia, December, 14AFMC Organizing Committee.

Wong, C. Y., Lanspeary, P.V., Nathan, G.J., Kelso, R.M. and O'Doherty, T. (2002). "Phase averaged velocity in a fluidic precessing jet nozzle and in the near external field", submitted to J. Experimental Thermal and Fluid Science, May.

Zaman, K. B. M. (1999). "Spreading characteristics of compressible jets from nozzles of various geometries", J. Fluid Mech., 383, pp.197-228.